Water Resources Research

RESEARCH ARTICLE
10.1029/2024WR038036

Carbon Emissions From Low-Order Streams in a Tropical, High-Elevation, Peatland Ecosystem Are Mediated by Catchment Morphology

Keridwen M. Whitmore[1], Amanda G. DelVecchia[1], Elizabeth Farquhar[2], Gerard Rocher-Ros[3], Esteban Suárez[4], and Diego A. Riveros-Iregui[1]

[1]Department of Geography, University of North Carolina at Chapel Hill, Chapel Hill, NC, USA, [2]Department of Civil, Construction, and Environmental Engineering, North Carolina State University, Raleigh, NC, USA, [3]Department of Forest Ecology and Management, Swedish University of Agricultural Sciences, Umeå, Sweden, [4]Laboratorio de Ecología Acuática, Instituto BIOSFERA, Universidad San Francisco de Quito, Quito, Ecuador

Key Points:

- Patterns of pCO_2 and CO_2 emissions in tropical, páramo streams are consistent and predictable
- Dense drainage networks compensate for narrow widths of small streams resulting in similar CO_2 emissions in very small and large streams
- Accurate estimations of CO_2 emissions from entire river networks must consider shallow groundwater and wetland contributions

Supporting Information:

Supporting Information may be found in the online version of this article.

Correspondence to:

K. M. Whitmore and D. A. Riveros-Iregui,
kriddie@unc.edu;
diegori@unc.edu

Citation:

Whitmore, K. M., DelVecchia, A. G., Farquhar, E., Rocher-Ros, G., Suárez, E., & Riveros-Iregui, D. A. (2025). Carbon emissions from low-order streams in a tropical, high-elevation, peatland ecosystem are mediated by catchment morphology. *Water Resources Research*, *61*, e2024WR038036. https://doi.org/10.1029/2024WR038036

Received 22 MAY 2024
Accepted 30 MAR 2025

Author Contributions:

Conceptualization: Keridwen M. Whitmore, Diego A. Riveros-Iregui
Data curation: Keridwen M. Whitmore, Amanda G. DelVecchia, Elizabeth Farquhar
Formal analysis: Keridwen M. Whitmore, Amanda G. DelVecchia, Gerard Rocher-Ros, Diego A. Riveros-Iregui
Funding acquisition: Keridwen M. Whitmore, Esteban Suárez, Diego A. Riveros-Iregui
Methodology: Keridwen M. Whitmore, Amanda G. DelVecchia, Elizabeth Farquhar, Gerard Rocher-Ros, Diego A. Riveros-Iregui

Abstract

Inland waters emit large amounts of carbon and are key players in the global carbon budget. Particularly high rates of carbon emissions have been reported in streams draining mountains, tropical regions, and peatlands. However, few studies have examined the spatial variability of CO_2 concentrations and fluxes occurring within these systems, particularly as a function of catchment morphology. Here we evaluated spatial patterns of CO_2 in three tropical, headwater catchments in relation to the river network and stream geomorphology. We measured dissolved carbon dioxide (pCO_2), aquatic CO_2 emissions, discharge, and stream depth and width at high spatial resolutions along multiple stream reaches. Confirming previous studies, we found that tropical headwater streams are an important source of CO_2 to the atmosphere. More notably, we found marked, predictable spatial organization in aquatic carbon fluxes as a function of landscape position. For example, pCO_2 was consistently high (>10,000 ppm) at locations close to groundwater sources and just downstream of hydrologically connected wetlands, but consistently low (<1,000 ppm) in high gradient locations or river segments with larger drainage areas. Taken together, our findings suggest that catchment area and stream slope are important drivers of pCO_2 and gas transfer velocity (k) in mountainous streams, and as such they should be considered in catchment-scale assessments of CO_2 emissions. Furthermore, our work suggests that accurate estimation of CO_2 emissions requires understanding of dynamics across the entire stream network, from the smallest seeps to larger streams.

Plain Language Summary

Carbon emissions, particularly emissions of CO_2, from river systems are significant to the global carbon cycle. A major challenge in the study of river systems is that CO_2 concentrations and rates of CO_2 off-gassing are known to differ greatly within single stream reaches. In our study, we examined streams in a carbon-rich landscape, the tropical páramo, to describe patterns of dissolved CO_2 in streams and CO_2 emissions from stream surfaces and to identify the drivers behind such patterns. We found CO_2 concentrations to be very high at spring heads and downstream of wetlands, and to be lower in the downstream direction. Stream CO_2 and rates of CO_2 emission were highest in smallest streams, but their relative importance decrease when stream width was considered. Our study highlights the importance of considering the entire stream network, including stream surface area and drainage patterns, when estimating CO_2 emissions from freshwater landscapes.

1. Introduction

Rivers and streams are active sites of carbon transport and transformation that link terrestrial carbon to the atmosphere and ocean (Aufdenkampe et al., 2011). Upon entering a river, organic and inorganic carbon may be transported downstream, transformed via biological, chemical, and physical processes, or emitted to the atmosphere as a gas. The magnitude of carbon emissions from rivers is significant with over 60% of terrestrial carbon being emitted from surface waters to the atmosphere, primarily as carbon dioxide (CO_2) (Regnier et al., 2022). Furthermore, running waters play an outsized role in CO_2 emissions; rivers are estimated to cover a quarter of the surface area (SA) of lakes and reservoirs, but to emit more than 5 times the CO_2-C per year (Raymond et al., 2013a).

Recent studies have emphasized the outsized importance of headwater streams within a stream network. Smaller streams have a greater interface with terrestrial environments, which results in higher carbon inputs from groundwater per unit area (Argerich et al., 2016; Downing et al., 2012; Hotchkiss et al., 2015). Though individual

Project administration: Esteban Suárez, Diego A. Riveros-Iregui
Resources: Esteban Suárez
Supervision: Keridwen M. Whitmore, Esteban Suárez, Diego A. Riveros-Iregui
Visualization: Keridwen M. Whitmore, Amanda G. DelVecchia, Diego A. Riveros-Iregui
Writing – review & editing: Keridwen M. Whitmore, Amanda G. DelVecchia, Elizabeth Farquhar, Gerard Rocher-Ros, Esteban Suárez, Diego A. Riveros-Iregui

headwater SA is smaller than SA of higher-order rivers, the sum of headwater stream reaches may be equal to or greater than large river SA, often resulting in higher total emissions from low-order streams (Wallin et al., 2018). In addition, SA of small streams may be much greater than previously thought, particularly in areas with dense stream networks such as the Andean-Amazon basin where river area has been underestimated by up to 67% (Allen & Pavelsky, 2018).

Site specific attributes such as catchment topography (e.g., Rocher-Ros et al., 2019) and land cover (e.g., Lauerwald et al., 2015) influence the source and magnitude of CO_2 flux entering a river, and consequently rate of CO_2 emissions. Because global estimates rely on local estimates of emission rates and water SA, ecosystems that receive less attention may be poorly constrained and even omitted from scientific understanding of the global carbon budget altogether (Cole et al., 2007; Lauerwald et al., 2015; Raymond et al., 2013a). As research of historically understudied ecosystems has increased, estimates of terrestrial carbon inputs to rivers and carbon emissions from rivers have been refined and, in general, increased (Drake et al., 2018). Recent studies have found that mountain streams support high CO_2 emission rates owing to their high turbulence (Horgby et al., 2019; Ulseth et al., 2019) and tropical systems are hotspots for CO_2 emissions due to high input of carbon from terrestrial ecosystems (Borges et al., 2015; Chiriboga & Borges, 2023). Thus, tropical mountain streams may exhibit some of the highest CO_2 emissions found in river systems worldwide, yet measurements in these environments are clearly lacking (Battin et al., 2009; Drake et al., 2018; Lauerwald et al., 2023; Raymond et al., 2013b; Riveros-Iregui et al., 2018).

High spatial variability of CO_2 emissions within catchments and river networks (Rocher-Ros et al., 2019; Wallin et al., 2018; Whitmore et al., 2021) poses a challenge for researchers seeking to generalize carbon emission and scale up measurements to ecosystem level. First order controls on CO_2 emissions from aquatic environments are: (a) dissolved CO_2 concentration (pCO_2) and (b) gas transfer velocity (k) which scales with near-surface water turbulence (Raymond et al., 2012; Zappa et al., 2007). While some studies measure CO_2 emission rates directly (e.g., Sawakuchi et al., 2017; Schneider et al., 2020), many studies calculate this flux from measurements of pCO_2 in water and measurements or models of k (Lundin et al., 2013; Raymond et al., 2013b; Schelker et al., 2016). Regardless of method, studies that couple catchment morphology, landscape position, measurements of pCO_2, and modeled or directly measured k and CO_2 emissions are rare; yet they are needed to understand the processes driving spatial patterns of pCO_2 emission across the freshwater landscape (Rocher-Ros et al., 2019). Direct observations are essential to gain mechanistic understanding of the role of geomorphology as a driver of spatial variability in aquatic carbon emissions within catchments.

Hydraulic geometry is a key characteristic of river systems and a primary control on k in flowing waters (Raymond et al., 2012). Our study takes place in the Ecuadorian páramo, a tropical mountain biome located approximately 3,500 m above sea level in the Northern Andes Mountains. Unlike temperate and boreal systems, the hydraulic geometry of páramo rivers remains largely unreported, presenting a challenge for researchers aiming to quantify carbon fluxes in these vital ecosystems. We aim to address this literature gap by reporting measurements of pCO_2, discharge, width and depth and by establishing empirical relationships between measurements and catchment size and channel slope. We have set the following objectives.

1. To report on emergent patterns of pCO_2 observed within páramo stream reaches, from upstream to downstream and from tributaries to receiving streams.
2. To determine the primary driver of CO_2 emissions in páramo headwater streams of varying sizes.
3. To establish empirical relationships between pCO_2, the hydraulic geometry of páramo rivers, catchment size, and stream slope, and to further use these relationships in upscaling estimates of CO_2 emission from three headwater catchments.
4. To evaluate patterns of emissions across páramo river networks, and how patterns differ across catchments.

In this study, we present estimates pCO_2, discharge, stream channel geomorphology and catchment size, either measured in the field or remotely, at high spatial resolutions along three river reaches and three small tributaries. Using measured pCO_2 and modeled k based on channel geomorphology, we present estimates of CO_2 emissions. We evaluate changes in pCO_2 from upstream to downstream and changes within the river network in relation to characteristics of stream slope and catchment area. We also use empirical relationships between field measurements and remotely sensed variables, catchment size and slope, to upscale CO_2 emission estimates to the river-networks of three adjacent headwater catchments. The new information provided here will enhance our

understanding of the spatial variability in aquatic carbon fluxes from inland waters and help us to constrain estimates of CO_2 emission from heterogeneous, headwater stream networks in the páramo.

2. Materials and Methods

2.1. Study Site

This study was located in a moist páramo ecosystem within Cayambe Coca National Park (0.0500°N, 77.8000°W), in the Eastern range of the Ecuadorian Andes. Páramo ecosystems form a discontinuous ecoregion found at high altitudes in the tropical Andes Mountains from Venezuela to northern Peru. Within our study site, high annual precipitation rates and u-shaped valleys carved by glacier activity have resulted in a complex freshwater landscape with high density of lakes and wetlands, and steep-sloped headwater streams, interrupted by frequent waterfalls (Josse et al., 2009). About 20% of this landscape is covered by peatlands, formed as a result of low temperatures, consistently high water-table levels, and elevated rates of primary production. Peatlands in this region support rich organic soils, with average depths of 3.8 m (Hribljan et al., 2017). Owing to these characteristics, páramo landscapes hold great potential for high rates of organic carbon loading and atmospheric carbon emissions.

A weather station managed by Fondo para la Protección del Agua is located at approximately the middle of our sample sites (0.3337°S, 78.1985°W; 4,345 m elev.), where it has recorded continuous weather data since 2007. Mean annual temperature at this location was 4.8°C and average annual precipitation accumulation was 1,527 mm —derived from 7 years with complete precipitation records. Our field campaign was conducted during the wettest months of the year (June through July). During this time, average daily precipitation accumulation was 4.9 mm d^{-1} and average air temperature was 3.1°C.

We measured pCO_2, wetted width, and depth in headwater streams draining three small, high-elevation catchments, Antenas, Gavilán, and Colmillo (Figure 1). Sampling for our study took place over the course of a few weeks and during daylight hours between 10 a.m. and 3 p.m. We measured mainstem streams from 450 to 1,236 m in length, and three small tributaries to the Gavilán mainstem, from 44 to 238 m in length. The Gavilán mainstem included both the inlet and the outlet of a large wetland and was treated as two separate stream reaches for the analyses detailed below. Our sampling effort included measurements from small spring heads draining 0.3 ha catchments to downstream locations that drained catchments up to 228 ha in area (Table 1). On average, pCO_2 measurements were taken 23–40 m apart (Table S1 in Supporting Information S1), whereas width and depth measurements were measured every 10 m in all streams. Sampling locations ranged from 3,893 to 4,393 m in elevation. This elevation range included differences in vegetation type and soil depth, typical in páramo systems. Higher elevations correspond with shallower soils and are dominated by cushion plants that shift to sedge and rush vegetation at lower elevations.

2.2. Instrumentation

We measured pCO_2 with an infrared gas-analyzing (IRGA) CO_2 sensor (GMP-252 and GMM-220 Vaisala, Helsinki, Finland), adapted for use in aquatic environments by sealing a polytetrafluorethylene (PTFE) sleeve as in Johnson et al. (2010) and Schneider et al. (2020). Polytetrafluorethylene tubing is semi-permeable, allowing CO_2 dissolved in the water to come into equilibrium with air inside the tubing. Infrared gas-analyzing sensors were powered by a 12 V battery and connected to an Omega voltmeter data logger (OM-CP-VOLT101A-2.5 V, Omega Engineering Inc., Norwalk, Connecticut) programmed to record data every 5 s. Sensors were placed in the water and allowed approximately 15 min to reach equilibrium, a process that could be visualized as approaching an asymptote. After reaching equilibrium, the final sensor measurements were reported following adjustment for temperature and pressure for the GMP-220 and only for pressure for the GMM-252 model which adjusts for temperature internally. Barometric pressure was recoded with a barometric pressure transducer (Solinst Barologgers, Georgetown, Ontario) recording measurements every 15 min. Water temperature was recorded using pressure transducer water level loggers that also measured water temperature (Solinst Levelogger Edge, Georgetown, Ontario; Hobo-U20 Onset Computer Corporation, Bourne, MA). When factory calibrated and previously unused IRGA sensors were placed in water at the same location, allowed to come to equilibrium, and adjusted for pressure and temperature, readings were within instrument error provided by manufacturer.

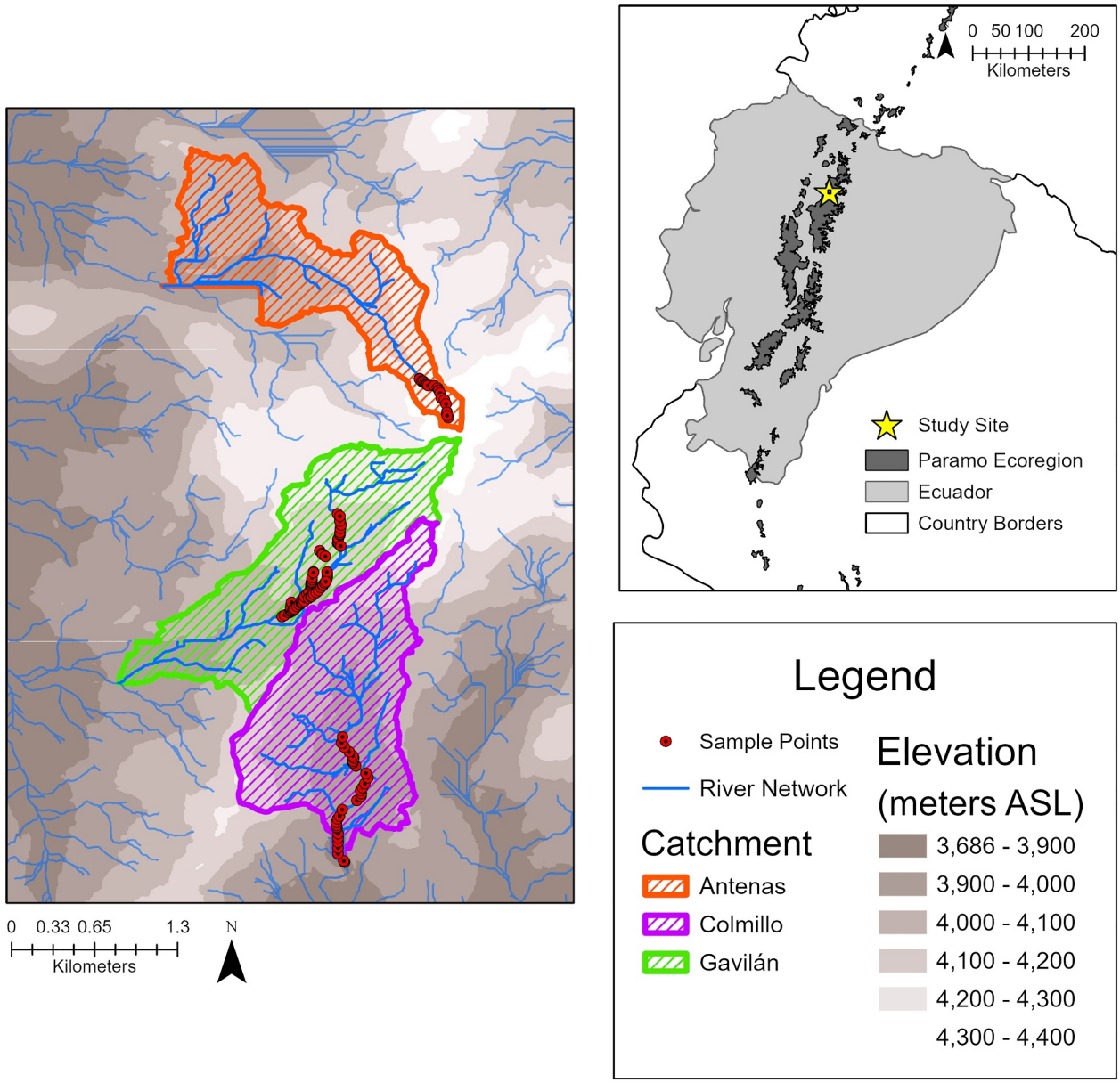

Figure 1. Location of pCO_2 measurements collected from 18 June 2021, to 9 July 2021, in headwater streams ranging 3,893 to 4,393 m above sea level in a páramo system in Cayambe Coca National Park, Ecuador. The river network was derived from a 3 m digital elevation model.

2.3. Geomorphology: Catchment Area and Slope

pCO_2 samples, wetted width, and depth measurements were geolocated using a handheld GPS unit (Garmin eTrex20, Olathe, KS) programmed to collect latitude, longitude, and elevation measurements every 10 s such that, as the researcher moved up and down the stream reach, the GPS unit recorded location data with maximum accuracy of 3 m. Waypoints were marked at each sample point and every 50 m to ensure accurate geolocation of width measurements. We identified stream flow paths by fitting a polynomial spline to the GPS recoded location data using the bs () function in the *R* "splines" package (Boergens et al., 2021; Hastie, 1992). Waypoints were snapped to the nearest point on the flow path prediction spline, thus adding attributes: latitude, longitude, distance, and elevation to all measurements (see Figures S1–S5 in Supporting Information S1).

We derived a flow accumulation raster using a 3 m resolution, digital terrain model (DTM) available for Ecuador through the Agricultural Public Information System of Ecuador. Pixels of high flow accumulation were

Table 1
Summary of Sample Point Location of Four Streams Reaches and Three Tributaries

Stream reach Units	Elevation Min (m)	Elevation Max (m)	Dates sampled	Catchment area (ha)	Ave. water temp. (°C)	Discharge at outlet (L/s)	Ave. slope (m/m)
Antenas	3,893	4,393	5–6 July	10.1	9.0	1.62	0.123
Colmillo	3,963	4,288	6–9 July	210.4	7.8	74.22	0.043
Gavilán	3,933	4,383					
Gavilán (wetland inlet)			29–30 June	41.6	8.1	1.01	0.166
Gavilán (wetland outlet)			18–22 June	108	8.2	15.17	0.093
Gavilán trib. 1			23–29 June	1.5	8.9	0.25	0.117
Gavilán trib. 2			23 June	18.2	10.0	0.305	0.085
Gavilán trib. 3			29 June	0.5	8.2	NA	0.067

determined to be within the flow path of our river network. The outlet of Gavilán flowed through a wide peatland where minimal elevation differences result in more uncertainty in flow path location. We found that the prediction spline developed for the outlet of the Gavilán wetland improved flow path location based on field observations. This was verified with RGB imagery of the site captured by drone (Mavic Pro V1, Da-Jiang Innovations, Nanshan District, Shenzhen). Flow accumulation was converted to catchment area in which each pixel was equal to 9 m^2. Sample locations were snapped to the nearest flow pathway. In this way, sample points were also associated with corresponding catchment area.

Slope was calculated as the difference in elevation between an upstream and downstream location divided by distance for each sample point and was determined two ways, (a) slope-mid is the elevation difference between 10 m downstream and 10 m upstream of a sample point and (b) slope-up is elevation difference between a measurement and 20 m upstream. This approach allowed us to estimate a slope value that was more representative of each measurement location considering the complexity of the terrain. We used elevation data from the DTM in combination with distance predicted by our river spline to calculate slope-mid and slope-up for all pCO_2, width and depth measurements. We calculated a slope of zero for 19 out of 113 pCO_2 measurement locations and 52 out of 284 width and depth measurement locations. Slope of zero was attributed to insufficient resolution of the DTM rather than reflecting the landscape. Consequently, these samples were assigned a value of 0.00025, or approximately half the detection limit of 0.01 m elevation difference divided by 20 m distance.

2.4. Discharge and Velocity

Stream gauging stations were established in streams, Gavilán and Colmillo where a water level-discharge rating curve was developed using a pressure transducer sensor (HOBO Water Level Data Logger, Onset Bourne, MA). Sensors recorded water level every 15 min and were paired with 20–23 discharge measurements using a handheld velocity probe (FH950 Portable Velocity Meter, Hach Company, Loveland, Colorado). Where continuous data was available, we report the average of all measurements recorded during sampling of a given stream. In streams that were not gaged, we collected a single discharge measurement using the handheld unit at or near the most upstream and most downstream location of each stream reach. We estimated discharge in unmeasured river segments by developing a relationship between catchment area and discharge. A total of 16 discharge measurements spanning the full range of catchment areas were collected. We calculated velocity (V, m s^{-1}) at locations were both width (w, m) and depth (D, m) measurements were collected using Equation 1 (Leopold & Maddock, 1953).

$$V = \frac{Q}{w \times D} \quad (1)$$

2.5. Calculating Gas Transfer Velocity and CO_2 Emission

Temperature-corrected gas transfer velocity (k_{600}) was estimated using a set of empirical equations provided by Ulseth et al. (2019), developed from measurements of stream hydraulics and geomorphology and tracer injection-

based k_{600} estimates. These researchers found k_{600} to scale with stream energy dissipation rate (eD, $m^2\ s^{-3}$) calculated as a product of gravitational acceleration (g, $m\ s^{-2}$), and stream hydraulic geometry variables, velocity, and slope (S, unitle ss) as described in Raymond et al. (2012) (Equation 2). We used DTM-derived slope and velocity calculated from Equation 1 as inputs to Equation 2. A piece-wise power-law with a breakpoint at $eD = 0.02$ (Equation 3) described 78% of variability in measured streams which included high gradient, mountain streams (Ulseth et al., 2019). In our study, 11% of the reaches sampled had at least one characteristic (i.e., discharge, velocity, slope, depth, or width) below the range of streams measured in Ulseth et al. (2019).

$$eD = g \times S \times V \tag{2}$$

$$\text{For } eD < 0.02\ \ln(k_{600}) = 0.35 \times \ln(eD) + 3.10$$

$$\text{For } eD > 0.02\ \ln(k_{600}) = 1.18 \times \ln(eD) + 6.43 \tag{3}$$

We derived k from k_{600} using the Schmidt number of 600 that corresponds to CO_2 at 20°C using coefficients provided in Wanninkhof (2014) (Equation 4). An exponent of 0.5 reflects the turbulent nature of running waters measured in this study (Zappa et al., 2007) (Equation 5). CO_2 emission, or flux (F_{CO2}) is the product of k and the concentration gradient between CO_2 in the water and CO_2 saturation with the atmosphere (Equation 6). The concentration of aqueous CO_2 was calculated as the product of pCO_2 measured in the field and Henry's Constant (K_H) adjusted for temperature using constants published in Sander (2023). The concentration of aqueous CO_2 at equilibrium with the atmosphere can be calculated as the partial pressure of CO_2 in the air ($pCO_{2\text{-air}}$) and Henry's Constant (K_H) (Raymond & Cole, 2001). While pCO_2 was measured directly, we used 416.45 ppm as a constant value for concentration of CO_2 in the air. This value is the average concentration measured by Mauna Loa Observatory (NOAA Earth System Research Laboratories Global Monitoring Laboratory) in 2021. In our study, CO_2 was not always recorded at the same interval as width and depth measurements, therefore we associated pCO_2 with each estimate of k_{600} by applying a linear interpolation between pCO_2 sample points.

$$SC_{CO_2} = -125.06 \times T_w + 4.3773 \times {T_w}^2 + 0.085681 \times {T_w}^3 + 0.00070284 \times {T_w}^4 \tag{4}$$

$$k_{600} = k \times \left(\frac{600}{Sc_{CO_2}}\right)^{-0.5} \tag{5}$$

$$F_{CO_2} = k \times (pCO_2 - pCO_{2-air}) \times K_H \tag{6}$$

To calculate SA of the stream, we used direct measurements of width taken in the field and distance between width measurements, which was 10 m for all streams. Total emission (F_{total} μmol d^{-1}) was calculated as a product of modeled emission (μmol $m^{-2}\ d^{-1}$) and SA (m^2) (Equation 7). These calculations were performed for each sub-reach.

$$F_{total} = F_{CO_2} \times SA \tag{7}$$

2.6. Statistical Analysis

We also tested distance from the most upstream measurement as a predictor of pCO_2 using linear regression. We used multiple log-linear regression models to test the relationship between our field observations (pCO_2, width, depth and discharge), and DTM derived spatial variables (catchment area and slope gradient). When one variable was not found to be significant, we removed that variable and applied the regression model again before reporting p-values. If both methods for calculating slope were significant within the model, we selected the slope that resulted in the greatest increase in model fit. Models were further used to upscale estimated emissions to a river network as described in the following section. We applied an Analysis of Variance test followed by post-hoc test, Tukey Honest Significant Differences, to identify differences in CO_2 evasion, k_{600}, and pCO_2 among stream reaches. pCO_2, CO_2 emission, discharge, width, depth, slope, and catchment area were log transformed before all analyses to fit model assumption of normality.

2.7. Upscaling Measurements to the River Network

To examine spatial patterns of CO_2 emissions across river networks, we upscaled estimates of pCO_2 and k_{600} to a river network draining three adjacent catchments. We estimated pCO_2 throughout the river network using a log-linear relationship between pCO_2, catchment area and slope. We calculated velocity using Equation 1, and modeled k_{600} using Equations 2 and 3. To enable comparison across river networks, we delineated catchments of similar sizes by expanding catchments Antenas and Gavilán to approximately the same size our largest catchment, Colmillo. This expansion had an impact on the resolution of our data as a 5 m^2 by 1 m resolution DTM covered about 10% of each catchment area. We converted all 5 m^2 raster pixels to point and used a spline to interpolate a 3 m^2 raster. This process retained a higher resolution in the x and y-axis, but the z-axis resolution (elevation), was lowered from 0.01 to 1 m for the full catchment. As a result, our detection limit for slope increased in all upscaled estimates to 0.025, or half the detection limit of 1 m elevation difference divided by 20 m distance.

Each catchment outlet (i.e., the most downstream river segment) was selected by locating flow accumulation approximately equal to our highest flow accumulation in our largest catchment, Colmillo. The stream initiation value (i.e., the most upstream river segment) was selected based on field observations and by visually inspecting drone imagery from our field site. In the field, three streams that drained catchments 0.3–1 ha in size were sampled up to their spring head. We also observed wet areas—including small ponds—in drone imagery of catchments of the same size. Because we were unable to determine from imagery whether the wet areas were flowing, we selected the more conservative 1 ha as our stream initiation value.

We calculated slope-mid and slope-up for each river segment, represented as a 3×3 pixel, within our modeled stream network, which included streams draining catchments from 1 to 202 ha in area. To determine slope-mid, we selected river segments upstream and downstream at distances between 9 m and $9 \times \sqrt{2}$ m and with flow accumulation values closest to those of the target river segment. Slope-up were determined similarly, using river segments between 18 m and $18 \times \sqrt{2}$ m in distance upstream of the target river segment. We then calculated elevation difference and distance between upstream and downstream points to derive slope.

Resulting river networks were composed of between 3,546 and 5,099 river segments, 3 m in length. Less than 5% of slopes were less than 0 and omitted from the dataset. Slopes were equal to 0 in 29% of measurements and subsequently converted to 0.025. We developed site-specific log-linear relationships between remotely derived catchment size and slope and field-measured depth, width, discharge, and pCO_2 to (a) predict pCO_2, (b) model k_{600} and (c) calculate CO_2 emission for each river segment. To interpret findings for each catchment, we log transformed catchment area and separated stream reaches by catchment area into 5 bins.

2.8. Software

All statistical analyses were performed in *R* (R Core Team, 2024, version 4.3.2) and visualizations were produced in ggplot2 (version 3.4.4) (Wickham, 2009). Spatial analyses were preformed using ArcGIS Pro software and the hydrology toolbox (Environmental Systems Research Institute Inc., Redlands, CA), and the sf package in *R* (Pebesma & Bivand, 2025).

3. Results

We observed a wide span of pCO_2 concentrations, ranging from 317 to 11,460 ppm. In three measurements, maximum concentration was higher than reported here, as pCO_2 exceeded what is measurable by our sensors (approximately 11,500 ppm after adjusting for pressure and temperature). Calculated k_{600} ranged from 6.4 to 621 m d^{-1}. CO_2 emission rate, calculated from pCO_2 and k_{600}, ranged from −0.14 to 42.5 mol m^{-2} day^{-1} (Table 2). pCO_2 decreased from upstream to downstream within our smallest reaches where the most upstream sampling point was close to the spring head and the stream flowed directly from groundwater. These reaches included Antenas (p-value = 0.011, $R^2 = 0.28$) and two tributaries (p-value = 0.25 and 0.05, $R^2 = 0.32$ and 0.57) (Figure 2b). Though not significant, a similar pattern of decreasing pCO_2 was observed in Gavilán Tributary 2. There was no discernible trend in pCO_2 along the entirety of Gavilán stream reach. However, when Gavilán was separated into two stream reaches, upstream and downstream of a large wetland bisecting the stream, we observed a similar trend of decreasing pCO_2 beginning at the outlet of the wetland (p-value <0.0001, $R^2 = 0.65$) (Figure 2b).

Differences in pCO_2, CO_2 emission, and k_{600} among all stream reaches were found to be statistically significant. Pair-wise comparisons showed significantly higher pCO_2 in very small tributaries in comparison to other stream

Table 2
Summary of pCO_2, CO_2 Emission and k_{600} Values

Stream reach	Mean	Stdev	Median	Min	Max	Observations
			pCO_2 (ppm)			
Antenas	2,071	2,646	1,210	317	11,460	19
Colmillo	1,033	219	1,011	701	1,385	29
Gavilán Inlet	904	335	812	497	1,557	13
Gavilán Outlet	1,933	2,049	859	444	7,592	24
Gavilán Trib 1	5,460	3,653	4,539	1,896	11,206	13
Gavilán Trib 2	2,115	1,012	1,740	1,405	3,574	4
Gavilán Trib 3	2,337	1,733	1,733	1,201	5,842	6
			Modeled k_{600} (m d^{-1})			
Antenas	41.2	64.5	18.7	6.4	342.5	39
Colmillo	35.7	60.4	16.9	6.5	479.6	131
Gavilán Inlet	124.3	120.4	99.5	14.5	508.2	19
Gavilán Outlet	122.4	157.4	44.8	6.4	621.0	55
Gavilán Trib 1	24.1	17.2	18.7	7.0	73.7	18
Gavilán Trib 2	46.1	27.4	39.9	16.9	91.8	8
Gavilán Trib 3	NA	NA	NA	NA	NA	NA
			Modeled CO_2 emissions (mol m^{-2} d^{-1})			
Antenas	2.63	5.04	0.94	0.099	23.4	39
Colmillo	1.50	2.51	0.72	0.20	20.2	131
Gavilán Inlet	4.22	4.96	2.53	0.67	20.6	19
Gavilán Outlet	6.58	11.6	2.76	0.074	72.4	55
Gavilán Trib 1	3.89	2.69	3.09	0.84	12.7	18
Gavilán Trib 2	3.71	3.18	2.63	1.24	10.9	8
Gavilán Trib 3	NA	NA	NA	NA	NA	NA

reaches (p-value <0.001 for all comparisons) (Figure 3a). k_{600} was significantly higher in Gavilán Inlet and Outlet than in Antenas, Gavilán tributaries and Colmillo (p-value <0.0003 for all comparisons) (Figure 3b). We found Gavilán outlet to support significantly higher CO_2 emission rates than Antenas (p-value <0.00001), and Colmillo (p-value = 0.0003) (Figure 3c). CO_2 emission from Gavilán Inlet was also significantly higher than Antenas (p-value = 0.006). CO_2 emission from Antenas was higher than Colmillo (p-value = 0.05). Taken together, the highest pCO_2 measurements were recorded in our smallest streams, whereas the highest k_{600} values were calculated for two mid-sized streams. Emissions were highest in our smallest streams and mid-sized streams.

We found hydraulic attributes, such as discharge, width, and depth to increase with catchment area. Logarithmic linear regressions between catchment and all hydraulic variables were highly significant (p-values <0.00001). Catchment area explained 70% of variation in discharge (Figure 4a) and 34% of variation in channel width (Figure 4b). Depth had a negative relationship with stream slope (p-value = < 0.0001). On average, steeper slopes yielded shallower rivers. Together, catchment and slope explained 51% of variance in depth (Figure 4c).

We found larger catchment area and steeper slopes to correlate with lower pCO_2. We found the slope 20 m above a sample point to be a better predictor of pCO_2 than 10 m above and 10 m below the sample point. Catchment size and stream slope explained 27% of variation in all pCO_2 measurements in our study sites (p-value <0.0001). Four measurements recorded downstream of a large wetland and upstream of a 10 m waterfall, a distance of 120 m, were much higher in pCO_2 than predicted by our multilinear regression. Removing these 4 measurements improved the model fit of the log-linear relationship from $R^2 = 0.27$ to $R^2 = 0.42$ (Figure 5).

To visualize emission differences along a river reach, we multiplied emission by SA and then calculated cumulative flux from the most upstream measurement to the most downstream reach (Figure 6). These estimates revealed that Gavilán outlet emitted more than five times the amount of CO_2 over a 300 m reach than the amount emitted from all other streams over a similar distance. This analysis also highlights the outsized contribution of specific river segments to total emission. For example, emissions that occurred between 80 and 110 m in Gavilán Outlet made up almost half of the emissions from the full reach sampled, 590 m in total. This stream segment corresponds to a tall waterfall downstream of a flow-through wetland. Similarly, emissions from within 50 m was equal to about a third of total emissions from Colmillo, a 1,350 m river reach.

Using the information above, we modeled pCO_2, k_{600}, and CO_2 emission for every 3 m length stream segment in river networks draining three catchments of approximately equal area. Models were based on the relationship

Table 3
Models Used to Calculate Hydraulic Geometry of Headwater Páramo Streams Including Intercept, Coefficients, and Estimate of Model Fit and Statistical Significance

Model	Intercept	ln (catchment)	ln (slope+1)[a]	R-sq	p-value
1. ln (Q_m3s) ~ ln (catchment)	−9.2275	1.1326	NA	0.70	<0.0001
2. ln(w) ~ ln (catchment)	3.16554	0.24332	NA	0.34	<0.0001
3. ln(d) ~ ln (catchment) + ln (slope+1)	1.49607	0.38943	−1.89478	0.51	<0.0001
4. ln (pCO2) ~ ln (catchment) + ln (slope+1)[b]	7.93443	−0.17284	−2.55674	0.27	<0.0001
5. ln (pCO2) ~ ln (catchment) + ln (slope+1)[c]	7.85000	−0.18424	−2.04810	0.42	<0.0001

[a]Slopes in model 3 was calculated using elevation difference 10 m upstream and 10 m downstream of the measurement point. Slope in models 4 and 5 was calculated using elevation difference between the measurement point and 20 m upstream. [b]This model includes all pCO_2 measurements collected. [c]This model omits pCO_2 measurements collected within a 120 m reach downstream of the large Gavilan wetland, and upstream of a 10 m waterfall.

10.1029/2024WR038036

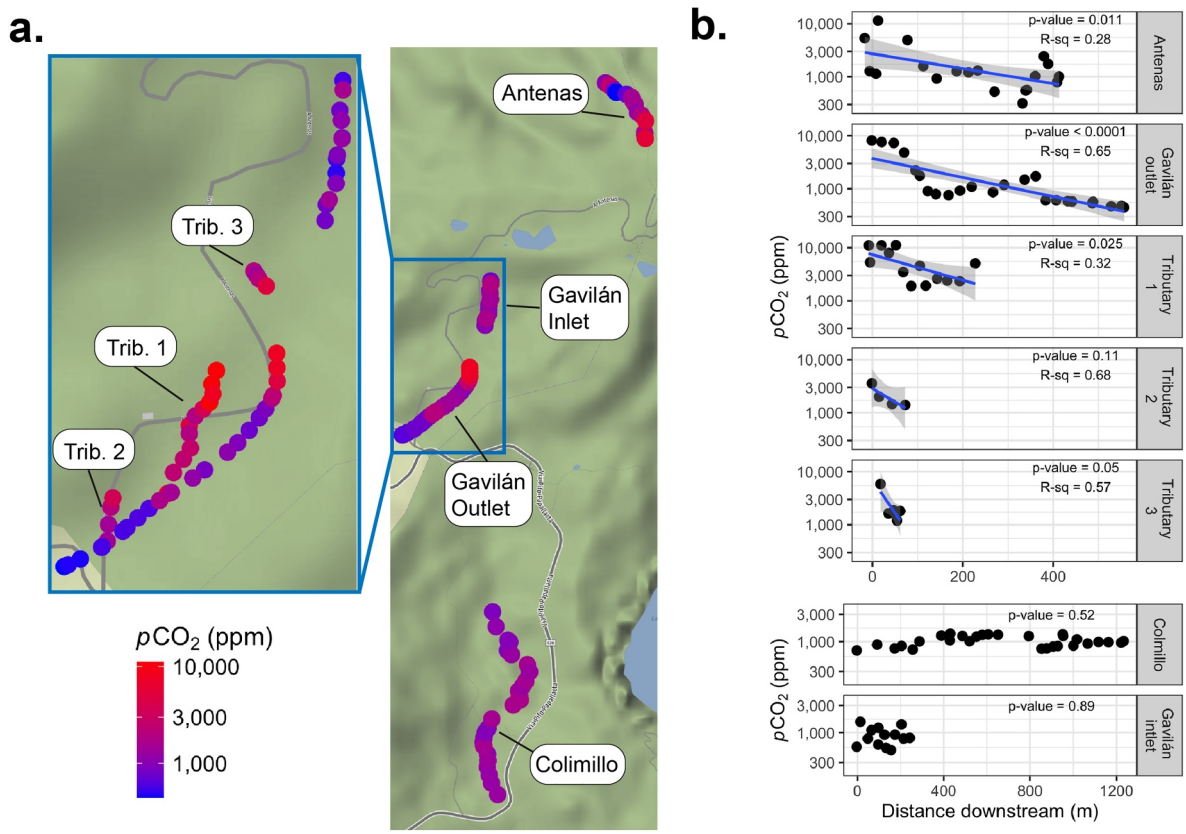

Figure 2. (a) The spatial distribution of pCO_2 measurements in all mainstream reaches and inset of the Gavilán river network with stream reaches labeled, and (b) Relationship between pCO_2 and distance downstream within river reaches. Distance of 0 indicates the most upstream measurement within a stream reach. Streams in which a significant downward trend was observed include Antenas, the outlet of the large in-stream wetland in Gavilán, and three Gavilán tributaries.

between catchment area, stream slope (derived from a DTM), and stream discharge, width, and depth as observed in the field. Our findings show that while pCO_2 decreases with increasing catchment area (Figure 7a), k_{600} increases with catchment area for the smallest and mid-sized catchment size bins although not across the largest catchments (Figure 7b). CO_2 emission declined slightly with catchment area for all catchments (Figure 7c). However, when stream width was accounted for in upscaled estimates, we observed a general trend of increasing CO_2 emission (mol d^{-1}) with catchment area (Figure 7d).

We evaluated CO_2 emission from an entire stream network (Figure 8a) by summing estimates of emission for each catchment area bin. As expected from a typical stream network, stream reaches draining small areas were more abundant than large streams (Figures 8b and 8c). In all stream networks, most CO_2 is evaded in our smallest streams. However, we did not observe consistent patterns of CO_2 emission among catchments. In the river network draining the Antenas catchment, total flux decreases with increasing catchment area. This pattern was not observed in the Gavilán catchment where emission was highest in both its smallest and largest catchment areas.

4. Discussion

Our study reports direct measurements of pCO_2 and hydraulic geometry of headwater streams in an ecosystem underrepresented in scientific literature, the Ecuadorian páramo (Mosquera et al., 2023). Further, we upscaled our measurements to estimate CO_2 emission across the stream networks of three headwater catchments in the páramo. Streams were supersaturated and a source of CO_2 to the atmosphere in all measurements. Discrete measurements ranged from near equilibrium with the atmosphere to over 10,000 ppm. Our measurements were within the range of measurements recorded at the same location in 2019 (Schneider et al., 2020; Whitmore et al., 2021) and measurements recorded from headwater streams in boreal landscapes at high latitudes, from Scotland (Dinsmore et al., 2010) to Sweden (Lundin et al., 2013) to Quebec, Canada (Campeau et al., 2014; Taillardat et al., 2022).

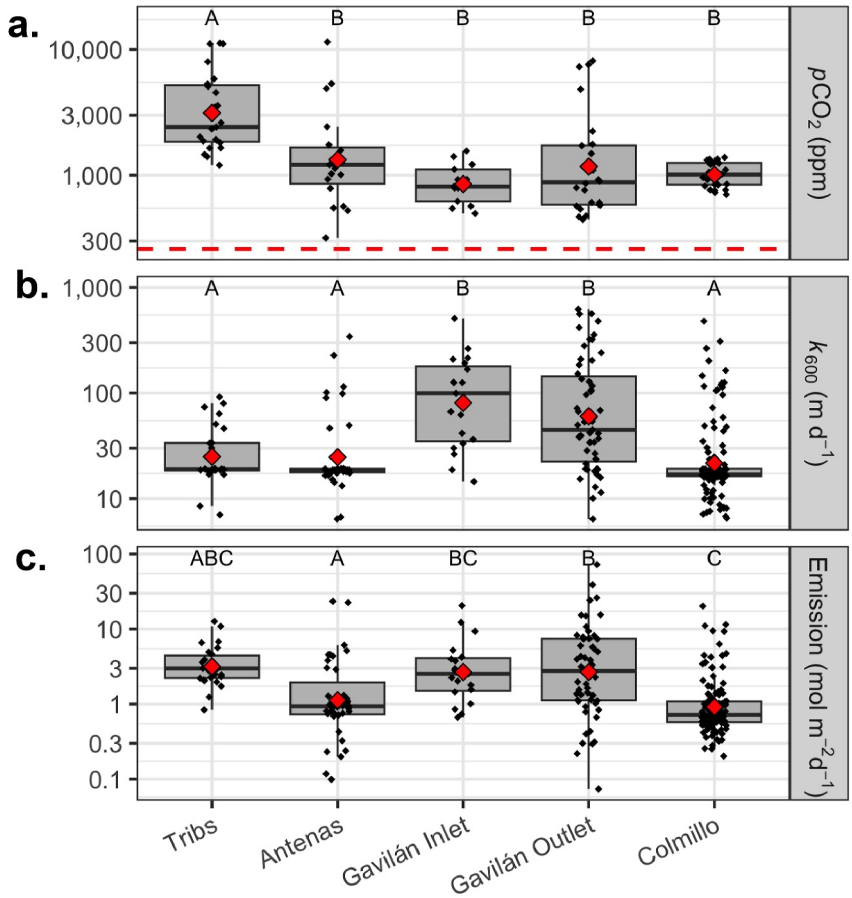

Figure 3. (a) Direct measurements of pCO_2, (b) calculated k_{600}, and (c) CO_2 emissions calculated from pCO_2 and k_{600} in four stream reaches, and from three small tributaries, arranged from smallest to largest in this figure. Letters indicate significant differences among stream reaches (p-value <0.05). Red diamonds indicate the mean values, and the dashed, red line indicates atmospheric CO_2 concentration.

pCO_2 recorded in our study's largest stream closely matched that of a first-order stream in northern Sweden, with average differences of less than 3% (Lundin et al., 2013). Though far from the tropics, the boreal landscapes highlighted in these studies shared similarities with our páramo site including glacier carved, U-shaped valleys, a high density of lakes and wetlands, and carbon rich, peatland soils. We found pCO_2 at our sites to be lower on average than in boreal studies. In addition, k_{600} values were higher in our study site as a result of steep slopes (Campeau et al., 2014; Lundin et al., 2013; Taillardat et al., 2022; Teodoru et al., 2009), and suggest that lower pCO_2 in our study region may be a result of faster emission rather than lower carbon loading.

pCO_2 reported in this study is much higher in both range and average than pCO_2 reported in studies of mountainous regions at northern latitudes such as in the Alps in Europe (mean = 718 ppm; Schelker et al., 2016) and the Rocky Mountains of North America (median = 445 ppm; Clow et al., 2021 and mean = 417 ppm; Crawford et al., 2015). In such studies, researchers report streams with steeply sloped catchments and dominated by rocky soils. Low pCO_2 in mountain streams has been attributed to low inputs from organic-carbon poor soils (Crawford et al., 2015). However, more recent studies have shown steep slopes of mountain streams drive high rates of emission and a rapid decline in pCO_2 rather than suppressed groundwater inputs (Clow et al., 2021; Horgby et al., 2019). In contrast, streams in our site are not only steep sloped but they also sustain pCO_2 concentrations well above atmosphere concentrations, >1,000, presumably due to shallow and subsurface groundwater inputs supplemented by in-stream respiration, as observed in other studies (Duvert et al., 2018; Horgby et al., 2019; Limpens et al., 2008).

Sampling for our study took place over the course of a few weeks and during daylight hours. This short but spatially explicit snapshot of pCO_2 dynamics does not account for diurnal or seasonal variation in temperature, light, and climate—all of which are expected to drive fluctuation in pCO_2 throughout the day and year. Globally,

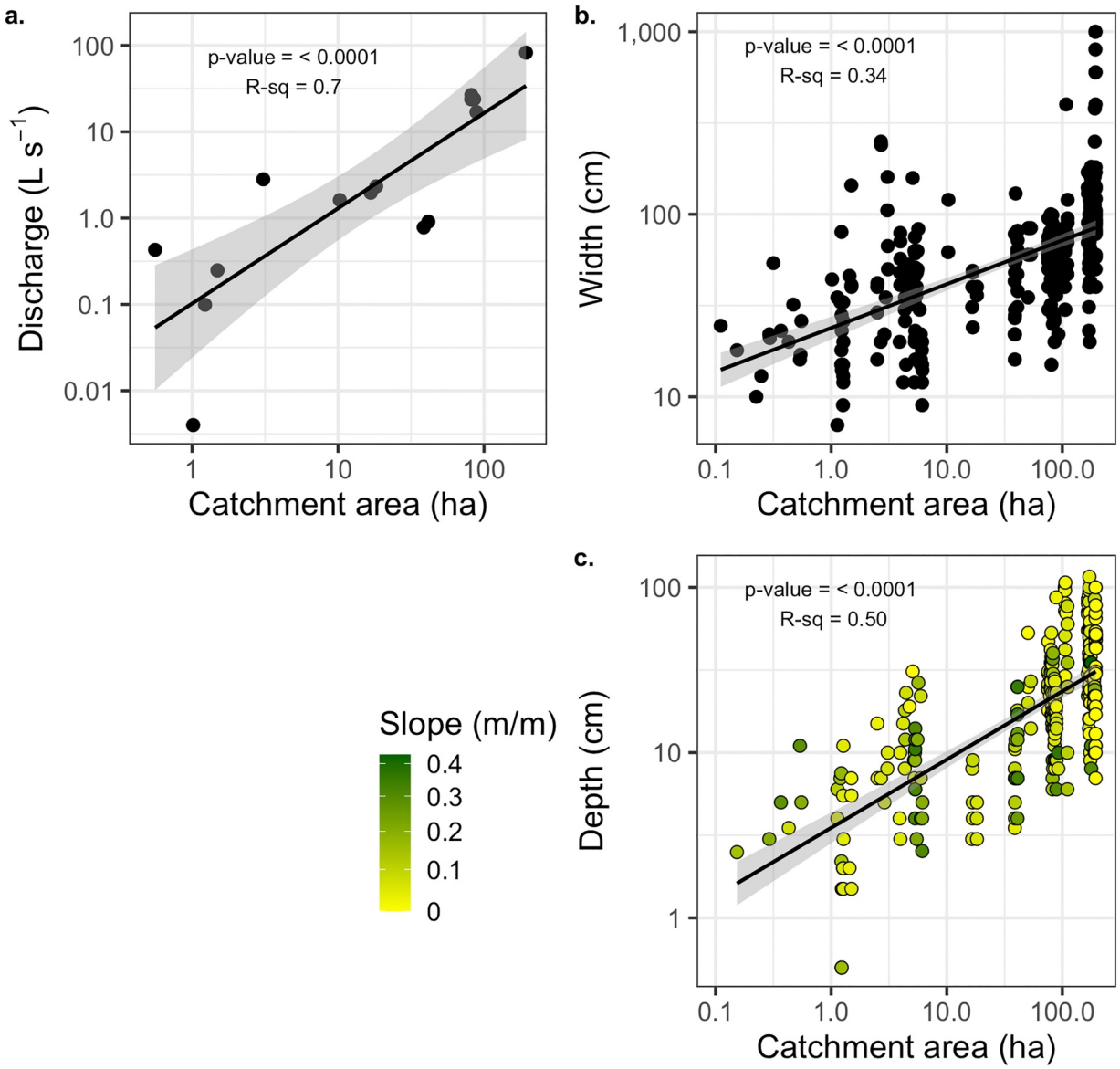

Figure 4. (a) Discharge, (b) width, and (c) depth increased with catchment area in a páramo river network. In addition, depth decreased with stream gradient (slope). The black line is the fit from natural log-linear regressions and the gray band represents 95% confidence interval of the predicted hydraulic variable. Coefficients for all models can be found in Table 3.

CO_2 emission from rivers increase at night, driven in part by biotic in-stream processes (Gómez-Gener et al., 2021), and by storm-events (Woodrow et al., 2024). A previous study of the Gavilán outlet reported maximum pCO_2 to occur most frequently at-dawn, which is also outside of our sampling window (Whitmore et al., 2021). Since our sampling effort took place from the late morning through the afternoon, we expect reported values of pCO_2 to be slightly lower than daily averages. Seasonally, the tropical páramo is far more consistent in temperature throughout the year than other systems at higher latitudes. Unlike boreal streams, páramo streams never accumulate ice and likely emit CO_2 year-round. Understanding the effect of seasonality is critical to accurately estimating carbon emissions from the tropical páramo and a major need in future sampling efforts.

4.1. What Patterns of pCO_2 Can Be Observed Within River Reaches and Within River Networks?

We observed a pattern of decreasing pCO_2 in the downstream direction in small stream reaches that originate at spring heads. Concentrations that exceeded 10,000 ppm decreased by over 70% within 100 m, a rate of decline

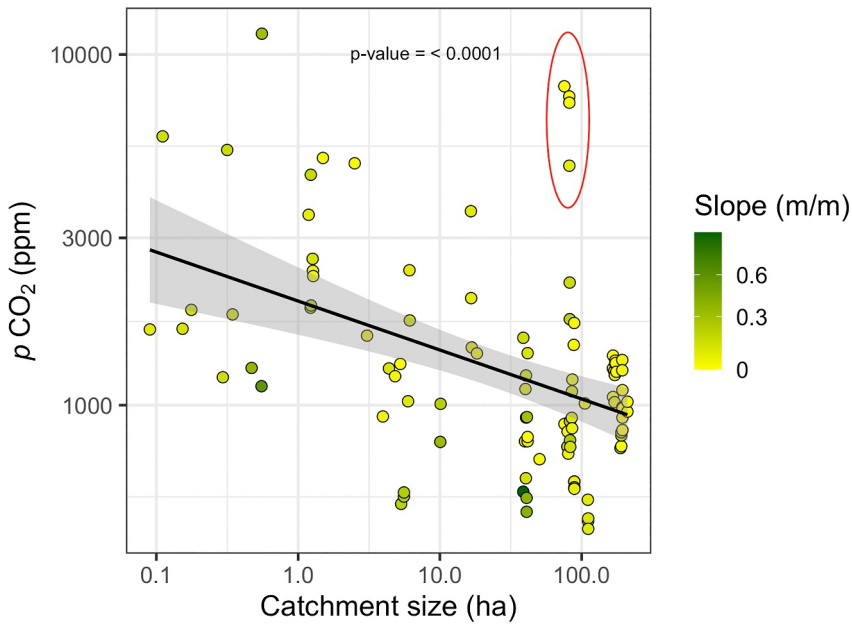

Figure 5. pCO_2 decreased with catchment area and with increasingly steep steam gradient upstream of sample point. The black line is the fit from log linear regressions and the gray band represents 95% CI of the predicted hydraulic variable. The red circle indicates 4 sample points measured directly below a large wetland outlet. Model fit improves with the removal of these points from $R^2 = 0.27$ to $R^2 = 0.42$. Coefficients for pCO_2 prediction model can be found in Table 3.

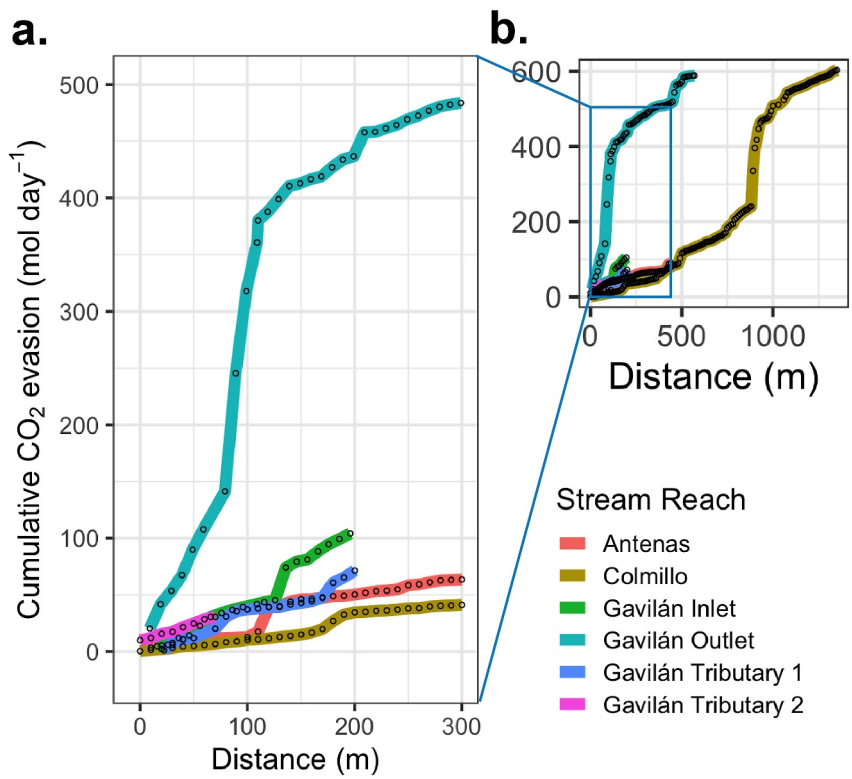

Figure 6. (a) Total cumulative emission from river reaches Antenas, Colmillo, Gavilán and two tributaries from the most upstream sample point to 300 m downstream, and (b) total cumulative emission for all reached sampled of variable lengths. Black circles indicate sample points every 10 m where k_{600} was modeled and emission calculated and represent the sum of total emissions (mol d^{-1}) from each previous river segment. Colored lines indicate the distance that each reach was measured.

10.1029/2024WR038036

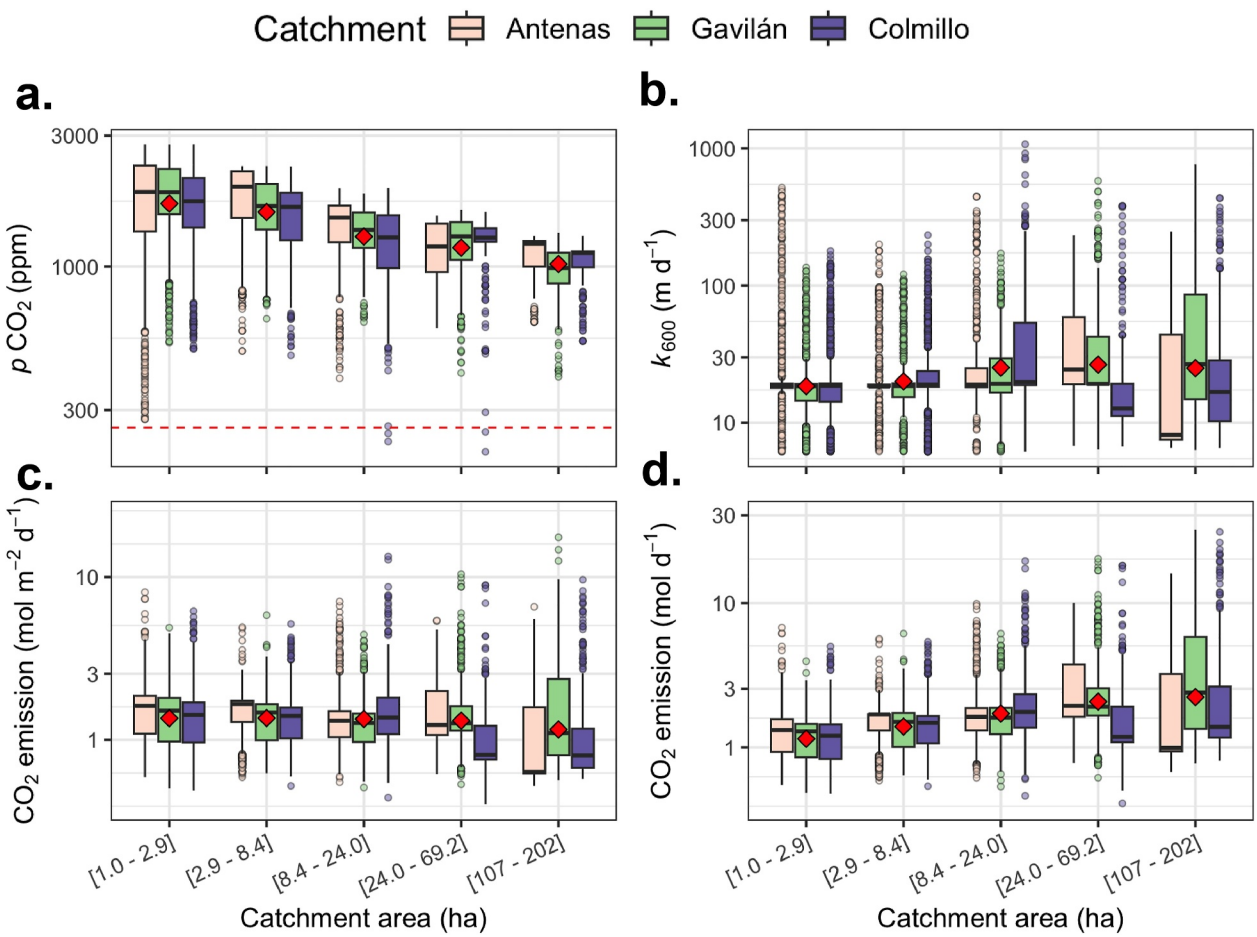

Figure 7. (a) pCO_2 in ppm, (b) k_{600} in m d^{-1}, (c) CO_2 emission in mol m^{-2} d^{-1}, and (d) CO_2 emission in mol d^{-1} modeled for all 3 m stream reaches within river networks of three similarly sized catchments, Antenas, Gavilán, and Colmillo. Stream reaches were separated into 5 bins following a logarithmic transformation of catchment area. Red diamonds indicate the mean value of all catchments for each sub-catchment area bin. Four negative values are not shown in Figures 7c and 7d due to log transformation.

within the range reported by other studies of pCO_2 attenuation in tropical, subtropical, and temperate seeps and springs (Chan et al., 2021; Duvert et al., 2018). A trend of decreasing pCO_2 with increasing stream size has been reported in previous studies (Finlay, 2003; Johnson et al., 2008; Wallin et al., 2018). For example, in a forested Amazonian catchment, very high pCO_2 concentrations were observed in seeps and headwaters in upstream locations (11,000 to 25,000 ppm), declining to 4,000 to 5,000 ppm within 5,000 m (Davidson et al., 2010).

A large, in-stream wetland interrupted the trend of declining pCO_2 in the Gavilán stream reach. Though pCO_2 concentrations at the inlet of the wetland were lower than 1,000 ppm, pCO_2 at the outlet was similar in magnitude to those observed at spring heads (~7,000 ppm). In addition, along the stream reach flowing out of the Gavilán, we observed short-lived increases in pCO_2 as the stream cut through a wetland and received lateral inflows of small tributaries (Figure 2b). Previous studies of peatland-rich environments have found pCO_2 to be closely related to soil type; for instance, pCO_2 is seen to decrease when flowing through mineral soil but increase when flowing through peatland soils (Hope et al., 2014; Wallin et al., 2010). As in our study, others have found peatland soils capable of replenishing CO_2 in streams to levels similar to direct additions from groundwater (Taillardat et al., 2022).

We observed the highest pCO_2 and the most pronounced downstream trend in areas where sampling points were close to groundwater springs or wetland outlets, highlighting the need to include springs and seeps in the evaluation of páramo river networks. We did not observe a trend of decreasing pCO_2 in our largest stream, Colmillo nor in the Gavilán Inlet. Though the most upstream measurement of Gavilán Inlet emerged from underground, our

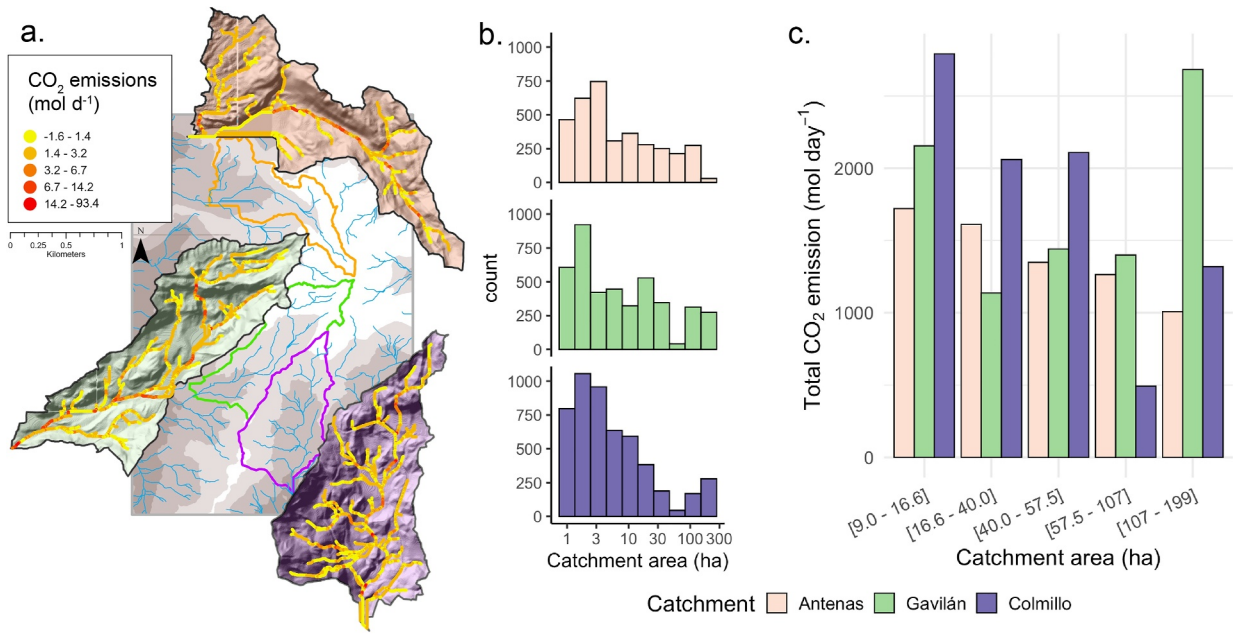

Figure 8. (a) Rate of CO_2 emission (mol d^{-1}) across the stream network of the three study catchments, (b) frequency distribution of catchment areas within the three study catchments, and (c) the total emission in mol day^{-1} for each sub-catchment area bin.

observations suggest the bulk of that flow comes from large macropore flowpaths, common in peatlands (Holden, 2005). In contrast with spring heads flowing from groundwater, macropore flowpaths can develop turbulent flow like those found in an open stream channel, capable of emitting CO_2 before reaching the macropore outlet (Dinsmore et al., 2011). Though lower in pCO_2 overall, stream reaches Colmillo and Gavilán Inlet did not reach equilibrium with the atmosphere (Figures 2 and 3a), and inputs from floodplains, riparian wetlands, and in-stream respiration are likely responsible for sustaining high pCO_2 throughout the reach (Duvert et al., 2018; Lupon et al., 2019, 2023).

Together, catchment area and stream slope were predictive of pCO_2 in streams. pCO_2 declined with catchment area and with steeper slopes upstream, explaining 42% variability in pCO_2. Previous studies have found slope to drive k in lotic environments (Raymond et al., 2012; Ulseth et al., 2019; Wallin et al., 2011) and thus we hypothesize that steeper slopes facilitate high emissions upstream and reduce pCO_2 downstream. pCO_2 in stream networks can be highly spatially variable (Rocher-Ros et al., 2019) and difficult to capture within heterogeneous river networks. An approach to representing this variability used a complex model that included groundwater inputs, water column, benthic hyporheic zone respiration, advection, and emission (Saccardi & Winnick, 2021), and even though model parameters were optimized to observations within their network, this model reached an R^2 of 0.70. A model based on global observation of pCO_2 that spanned wide gradients in productivity, biomes, and temperature and included many model predictors (Lauerwald et al., 2015) had an R^2 of 0.47. While our model is quite parsimonious, including only 2 predictors, it explains a substantial amount of variability of pCO_2 in our study system.

We identified pCO_2 measured just downstream of the Gavilán wetland to be outliers, underestimated by catchment and slope. The Gavilán wetland is a particularly large flow-through wetland that was not observed in any of the other catchments we sampled. We subsequently removed these points from upscaling models. Nonetheless, wetlands of this size do occur throughout the páramo and are clearly a substantial source of CO_2 to the atmosphere. Future work to upscale CO_2 estimates will need to include these uniquely large landscape features.

4.2. What Patterns of k_{600} Can Be Observed Within River Networks?

In our focal stream reaches, modeled k_{600} was highest in streams of intermediate size, namely the Gavilán inlet and outlet (Figure 3b). When we upscaled estimates to headwater river networks, our modeled estimation of k_{600}

also increased with catchment area from the smallest to mid-sized catchments. Modeled k_{600} was highest on average in our intermediate to largest streams but this trend varied greatly between catchments (Figure 7b). The increase in k_{600} with stream size was unexpected and differed from previous studies of both mountainous and low gradient landscapes (Clow et al., 2021; Raymond et al., 2012; Schelker et al., 2016; Wallin et al., 2018). Low order streams often correspond with steeper slopes, especially in mountainous environments. Findings of increasing k_{600} with stream size are rare. Campeau et al. (2014) for example, found increasing k_{600} with total stream length and attributed this to their boreal system's flat landscape.

Variability in discharge rather than slope was determined to be an important driver of k_{600} in our system. In this mountain environment, streams slopes were high in catchments of all sizes (Figure S6 in Supporting Information S1). In contrast, discharge, width, and depth, had a much stronger relationship to catchment area (Figure 4). While streams in this study range in size, they are all low-order streams. Had our study included larger streams we may have observed more consistently lower-gradient steam slopes.

It is important to note that the empirical relationships used to estimate k_{600} in our study are based on measurements made in non-páramo streams (Ulseth et al., 2019), which may differ in morphology, topography, and streambed roughness. In addition, the smallest streams measured in our study were smaller than the range of streams used to develop the Ulseth et al. (2019) models. Nonetheless, our measurements confirm that very small streams are capable of sustaining very high rates of CO_2 emission and therefore more accurate quantification of CO_2 emission in small systems is needed, not just in the páramo but globally. Furthermore, direct measurements of k_{600} that capture the role of microtopography within a single stream are needed. Direct observations using tracer injections of argon, propane, or CO_2 (Hall & Madinger, 2018; McDowell & Johnson, 2018) should be a focus of future work.

4.3. Where do Most Emissions Occur Within a Headwater River Network?

We highlight four factors central to understanding and upscaling CO_2 emission from a freshwater landscape. These factors can be thought of as iterative in nature, and include: (a) pCO_2, (b) k_{600}, (c) SA, and (d) density of the river drainage network. We found the interpretation of emission patterns and location of emission hotspots to change depending on the role of one or more of these factors. The highest emission rates per meter squared were observed in streams that drained catchments less than 50 ha in area. The outsized importance of small streams within a river network has been reported in many studies (Hotchkiss et al., 2015; Marx et al., 2017). Though all streams measured in this study are small, our analysis nevertheless shows the importance of considering SA. When we incorporated SA into our estimation of emission, small streams decreased in relative importance. A wider stream with greater water/atmosphere interface will emit more CO_2 than a narrower stream with comparable pCO_2 and k_{600} attributes and therefore we found emission rates to be generally higher in our larger streams (Figures 6 and 7). This may be particularly relevant to páramo systems, where elevated pCO_2 is sustained by groundwater inputs from carbon rich peatlands along the way in contrast to other systems where CO_2 may be more depleted in high order streams.

Lastly, in a dendritic drainage network, the density of smaller streams is higher than larger streams. Small streams have been found to make up 90% of total stream length in a Swedish catchments less than 15,000 m^2 (Bishop et al., 2008) and 96% of the number of streams globally (Marx et al., 2017). For our study region, the Andean-Amazon basin, it has been estimated that stream area has been underestimated by up to 67% because of small streams (Allen & Pavelsky, 2018). When we included the drainage network in our upscaled estimates of CO_2 emission from three catchments, we found the smallest streams to emit the highest amount of CO_2. Furthermore, we found catchment geomorphology, which shapes both drainage patterns and river gradient, to play an important role in determining where most emissions occur. As a result, we observed differences in the spatial patterns of total CO_2 emissions among catchments.

The upscaling exercise presented in this study omits atypical landscape elements such as large, flow-through wetlands. We have evidence that wetlands export high levels of pCO_2, not well predicted by catchment area and may contribute disproportionally to emissions from a catchment (Figure 6). Abrupt changes in elevation such as waterfalls or very steep reaches are also not fully represented in our upscaling model and may play an important role in controlling the location of emission hot spots within a catchment. We observed notable increases in CO_2 emission over short distances that corresponded to known locations of waterfalls (Figure 6). This finding is valuable in highlighting the potential disproportionate importance of localized points in driving CO_2 emissions.

Further, defining the spring head of a stream and predicting its location within the landscape can alter emission estimates greatly. Given that we omitted flow-through wetlands and used a conservative stream initiation value, we expect our estimate of emissions to be conservative overall. Finally, an elevation driven gradient of soil depth and vegetation community had the potential to be a confounding factor in our study where the elevation relief within each catchment is greater than 400 m. We saw no evidence of an elevation effect in our study: Antenas was very high in elevation, yet pCO_2 at its spring head was of similar magnitude to a same-sized stream at lower elevation. Nevertheless, future upscaling of this ecoregion should include consideration of flow-through wetlands, a more well-defined stream initiation value, and the potential effects of elevation and corresponding vegetation zones.

5. Conclusion

Our study, located in a high elevation, tropical peatland, represents a significant contribution to the body of literature estimating global carbon emissions from freshwater systems. Current global models rely on local estimation of carbon processes and surface water extent, which are critically lacking in páramo ecoregions. In this study we recorded direct measurements of pCO_2 and channel geometry in headwaters of a páramo ecosystem, evaluated spatial patterns across the landscape, and connected patterns to landscape geomorphology and riverine morphology.

We found streams to be net sources of carbon and measured very high pCO_2 at spring heads and at a wetland outlet. A pattern of decreasing pCO_2 within short distances underscores the importance of sampling headwaters near spring heads and at wetland outlets. Downstream, pCO_2 was sustained in larger rivers by some combination of floodplain soils, wetlands, and instream respiration. Decreasing pCO_2 and increasing k_{600} with catchment area resulted in CO_2 emission controls differing by landscape position. When we include SA, the largest stream appeared to become a more significant source of CO_2 emission. However, this gap closed when we considered the entire drainage network.

Our study highlights the need to include all components of the river network, rates of emission, stream width, and drainage network density when studying river systems. The spatially explicit observations presented here suggest that important contributions of dissolved carbon from shallow groundwater and peatlands along stream reaches are responsible for sustaining emissions across the stream network. However, our study represents only a starting framework. New research questions in combination with co-located, independent methodologies are needed to fully characterize carbon emission dynamics from these high-density páramo river networks. Future studies should focus on, for example, improved estimations of k_{600} in relation to geomorphology, independent, land-atmosphere measures of carbon exchange (e.g., eddy covariance), and the temporal variability of many of the dynamics presented here through continuous monitoring. Site specific models of k_{600} that include super saturated, very small streams are also needed. This information is important to inform models of CO_2 emissions to upscaled to entire river networks in tropical mountainous regions.

Data Availability Statement

All data used in analyses and figure production for this study are publicly available for download via HydroShare (Whitmore et al., 2024).

Acknowledgments
This work was supported by the U.S. National Science Foundation Grants EAR-1847331 and EAR-2317854, The Geological Society of America and The Society of Wetland Scientists Student Research Grants. DAR-I was supported by the U.S. Fulbright Scholar Program of the U.S. Department of State while writing this manuscript. We would like to thank the staff at the University of San Francisco Quito (USFQ) for logistical support as well as the communities of Cumbayá and Quito, Ecuador. We thank the Ministry of the Environment of Ecuador (research permit # 014-018-IC-FLO-DPAN/MA) and the National System of Protected Areas of Ecuador for site access. We thank two anonymous reviewers and the editors for comments and suggestions which greatly improved this manuscript.

References

Allen, G. H., & Pavelsky, T. M. (2018). Global extent of rivers and streams. *Science*, *361*(6402), 585–588. https://doi.org/10.1126/science.aat0636

Argerich, A., Haggerty, R., Johnson, S. L., Wondzell, S. M., Dosch, N., Corson-Rikert, H., et al. (2016). Comprehensive multiyear carbon budget of a temperate headwater stream. *Journal of Geophysical Research: Biogeosciences*, *121*(5), 1306–1315. https://doi.org/10.1002/2015JG003050

Aufdenkampe, A. K., Mayorga, E., Raymond, P. A., Melack, J. M., Doney, S. C., Alin, S. R., et al. (2011). Riverine coupling of biogeochemical cycles between land, oceans, and atmosphere. *Frontiers in Ecology and the Environment*, *9*(1), 53–60. https://doi.org/10.1890/100014

Battin, T. J., Luyssaert, S., Kaplan, L. A., Aufdenkampe, A. K., Richter, A., & Tranvik, L. J. (2009). The boundless carbon cycle. *Nature Geoscience*, *2*(9), 598–600. Article 9. https://doi.org/10.1038/ngeo618

Bishop, K., Buffam, I., Erlandsson, M., Fölster, J., Laudon, H., Seibert, J., & Temnerud, J. (2008). Aqua Incognita: The unknown headwaters. *Hydrological Processes*, *22*(8), 1239–1242. https://doi.org/10.1002/hyp.7049

Boergens, E., Schmidt, M., & Seitz, F. (2021). The use of B-splines to represent the topography of river networks. *GEM - International Journal on Geomathematics*, *12*(1), 21. https://doi.org/10.1007/s13137-021-00188-w

Borges, A. V., Darchambeau, F., Teodoru, C. R., Marwick, T. R., Tamooh, F., Geeraert, N., et al. (2015). Globally significant greenhouse-gas emissions from African inland waters. *Nature Geoscience*, *8*(8), 637–642. https://doi.org/10.1038/ngeo2486

Campeau, A., Lapierre, J.-F., Vachon, D., & del Giorgio, P. A. (2014). Regional contribution of CO2 and CH4 fluxes from the fluvial network in a lowland boreal landscape of Québec. *Global Biogeochemical Cycles*, *28*(1), 57–69. https://doi.org/10.1002/2013GB004685

Chan, C. N., Tsang, C. L., Lee, F., Liu, B., & Ran, L. (2021). Rapid loss of dissolved CO2 from a subtropical steep headwater stream. *Frontiers in Earth Science*, *9*. https://doi.org/10.3389/feart.2021.741678

Chiriboga, G., & Borges, A. V. (2023). Andean headwater and piedmont streams are hot spots of carbon dioxide and methane emissions in the Amazon basin. *Communications Earth & Environment*, *4*(1), 1–13. https://doi.org/10.1038/s43247-023-00745-1

Clow, D. W., Striegl, R. G., & Dornblaser, M. M. (2021). Spatiotemporal dynamics of CO2 gas exchange from headwater mountain streams. *Journal of Geophysical Research: Biogeosciences*, *126*(9), e2021JG006509. https://doi.org/10.1029/2021JG006509

Cole, J. J., Prairie, Y. T., Caraco, N. F., McDowell, W. H., Tranvik, L. J., Striegl, R. G., et al. (2007). Plumbing the global carbon cycle: Integrating inland waters into the terrestrial carbon budget. *Ecosystems*, *10*(1), 172–185. https://doi.org/10.1007/s10021-006-9013-8

Crawford, J. T., Dornblaser, M. M., Stanley, E. H., Clow, D. W., & Striegl, R. G. (2015). Source limitation of carbon gas emissions in high-elevation mountain streams and lakes. *Journal of Geophysical Research: Biogeosciences*, *120*(5), 952–964. https://doi.org/10.1002/2014JG002861

Davidson, E. A., Figueiredo, R. O., Markewitz, D., & Aufdenkampe, A. K. (2010). Dissolved CO2 in small catchment streams of eastern amazonia: A minor pathway of terrestrial carbon loss. *Journal of Geophysical Research*, *115*(G4). https://doi.org/10.1029/2009JG001202

Dinsmore, K. J., Billett, M. F., Skiba, U. M., Rees, R. M., Drewer, J., & Helfter, C. (2010). Role of the aquatic pathway in the carbon and greenhouse gas budgets of a peatland catchment. *Global Change Biology*, *16*(10), 2750–2762. https://doi.org/10.1111/j.1365-2486.2009.02119.x

Dinsmore, K. J., Smart, R. P., Billett, M. F., Holden, J., Baird, A. J., & Chapman, P. J. (2011). Greenhouse gas losses from peatland pipes: A major pathway for loss to the atmosphere? *Journal of Geophysical Research*, *116*(G3), G03041. https://doi.org/10.1029/2011JG001646

Downing, J. A., Cole, J. J., Duarte, C. M., Middelburg, J. J., Melack, J. M., Prairie, Y. T., et al. (2012). Global abundance and size distribution of streams and rivers. *Inland Waters*, *2*(4), 229–236. https://doi.org/10.5268/iw-2.4.502

Drake, T. W., Raymond, P. A., & Spencer, R. G. M. (2018). Terrestrial carbon inputs to inland waters: A current synthesis of estimates and uncertainty. *Limnology and Oceanography Letters*, *3*(3), 132–142. https://doi.org/10.1002/lol2.10055

Duvert, C., Butman, D. E., Marx, A., Ribolzi, O., & Hutley, L. B. (2018). CO2 evasion along streams driven by groundwater inputs and geomorphic controls. *Nature Geoscience*, *11*(11), 813–818. https://doi.org/10.1038/s41561-018-0245-y

Finlay, J. C. (2003). Controls of streamwater dissolved inorganic carbon dynamics in a forested watershed. *Biogeochemistry*, *62*(3), 231–252. https://doi.org/10.1023/A:1021183023963

Gómez-Gener, L., Rocher-Ros, G., Battin, T., Cohen, M. J., Dalmagro, H. J., Dinsmore, K. J., et al. (2021). Global carbon dioxide efflux from rivers enhanced by high nocturnal emissions. *Nature Geoscience*, *14*(5), 289–294. https://doi.org/10.1038/s41561-021-00722-3

Hall, R. O., Jr., & Madinger, H. L. (2018). Use of argon to measure gas exchange in turbulent mountain streams. *Biogeosciences*, *15*(10), 3085–3092. https://doi.org/10.5194/bg-15-3085-2018

Hastie, T. J. (1992). Generalized additive models. In *Statistical models in S*. Routledge.

Holden, J. (2005). Peatland hydrology and carbon release: Why small-scale process matters. *Philosophical Transactions of the Royal Society A: Mathematical, Physical & Engineering Sciences*, *363*(1837), 2891–2913. https://doi.org/10.1098/rsta.2005.1671

Hope, A. J., McDowell, W. H., & Wollheim, W. M. (2014). Ecosystem metabolism and nutrient uptake in an urban, piped headwater stream. *Biogeochemistry*, *121*(1), 167–187. https://doi.org/10.1007/s10533-013-9900-y

Horgby, A., Segatto, P. L., Bertuzzo, E., Lauerwald, R., Lehner, B., Ulseth, A. J., et al. (2019). Unexpected large evasion fluxes of carbon dioxide from turbulent streams draining the world's mountains. *Nature Communications*, *10*(1), 1–9. https://doi.org/10.1038/s41467-019-12905-z

Hotchkiss, E. R., Hall Jr, R. O., Sponseller, R. A., Butman, D., Klaminder, J., Laudon, H., et al. (2015). Sources of and processes controlling CO 2 emissions change with the size of streams and rivers. *Nature Geoscience*, *8*(9), 696–699. Article 9. https://doi.org/10.1038/ngeo2507

Hribljan, J. A., Suarez, E., Bourgeau-Chavez, L., Endres, S., Lilleskov, E. A., Chimbolema, S., et al. (2017). Multidate, multisensor remote sensing reveals high density of carbon-rich mountain peatlands in the páramo of Ecuador. *Global Change Biology*, *23*(12), 5412–5425.

Johnson, M. S., Billett, M. F., Dinsmore, K. J., Wallin, M., Dyson, K. E., & Jassal, R. S. (2010). Direct and continuous measurement of dissolved carbon dioxide in freshwater aquatic systems—method and applications. *Ecohydrology: Ecosystems, Land and Water Process Interactions, Ecohydrogeomorphology*, *3*(1), 68–78. https://doi.org/10.1002/eco.95

Johnson, M. S., Lehmann, J., Riha, S. J., Krusche, A. V., Richey, J. E., Ometto, J. P. H. B., & Couto, E. G. (2008). CO2 efflux from Amazonian headwater streams represents a significant fate for deep soil respiration. *Geophysical Research Letters*, *35*(17). https://doi.org/10.1029/2008GL034619

Josse, C., Cuesta, F., Navarro, G., Barrena, V., Cabrera, E., Chacón-Moreno, E., et al. (2009). Ecosistemas de los Andes del Norte y Centro. Bolivia, Colombia, Ecuador, Perú y Venezuela. In *Secretaría General de la Comunidad Andina, Programa Regional ECOBONA-Intercooperation, CONDESAN-Proyecto Páramo Andino, Programa BioAndes, EcoCiencia, NatureServe, IAvH*. LTA-UNALM, ICAE-ULA, CDC-UNALM, RUMBOL SRL.

Lauerwald, R., Allen, G. H., Deemer, B. R., Liu, S., Maavara, T., Raymond, P., et al. (2023). Inland water greenhouse gas budgets for RECCAP2: 1. State-Of-The-Art of global scale assessments. *Global Biogeochemical Cycles*, *37*(5), e2022GB007657. https://doi.org/10.1029/2022GB007657

Lauerwald, R., Laruelle, G. G., Hartmann, J., Ciais, P., & Regnier, P. A. G. (2015). Spatial patterns in CO2 evasion from the global river network. *Global Biogeochemical Cycles*, *29*(5), 534–554. https://doi.org/10.1002/2014GB004941

Leopold, L. B., & Maddock, T., Jr. (1953). The hydraulic geometry of stream channels and some physiographic implications. In Professional paper *(252)*. U.S. Government Printing Office. https://doi.org/10.3133/pp252

Limpens, J., Berendse, F., Blodau, C., Canadell, J. G., Freeman, C., Holden, J., et al. (2008). Peatlands and the carbon cycle: From local processes to global implications – A synthesis. *Biogeosciences*, *5*(5), 1475–1491. https://doi.org/10.5194/bg-5-1475-2008

Lundin, E. J., Giesler, R., Persson, A., Thompson, M. S., & Karlsson, J. (2013). Integrating carbon emissions from lakes and streams in a subarctic catchment. *Journal of Geophysical Research: Biogeosciences*, *118*(3), 1200–1207. https://doi.org/10.1002/jgrg.20092

Lupon, A., Denfeld, B. A., Laudon, H., Leach, J., Karlsson, J., & Sponseller, R. A. (2019). Groundwater inflows control patterns and sources of greenhouse gas emissions from streams. *Limnology & Oceanography*, *64*(4), 1545–1557. https://doi.org/10.1002/lno.11134

Lupon, A., Gómez-Gener, L., Fork, M. L., Laudon, H., Martí, E., Lidberg, W., & Sponseller, R. A. (2023). Groundwater-stream connections shape the spatial pattern and rates of aquatic metabolism. *Limnology and Oceanography Letters*, *8*(2), 350–358. https://doi.org/10.1002/lol2.10305

Marx, A., Dusek, J., Jankovec, J., Sanda, M., Vogel, T., van Geldern, R., et al. (2017). A review of CO2 and associated carbon dynamics in headwater streams: A global perspective. *Reviews of Geophysics*, *55*(2), 560–585. https://doi.org/10.1002/2016RG000547

McDowell, M. J., & Johnson, M. S. (2018). Gas transfer velocities evaluated using carbon dioxide as a tracer show high streamflow to be a major driver of total CO2 evasion flux for a headwater stream. *Journal of Geophysical Research: Biogeosciences*, *123*(7), 2183–2197. https://doi.org/10.1029/2018jg004388

Mosquera, G. M., Hofstede, R., Bremer, L. L., Asbjornsen, H., Carabajo-Hidalgo, A., Célleri, R., et al. (2023). Frontiers in páramo water resources research: A multidisciplinary assessment. *Science of The Total Environment*, *892*, 164373. https://doi.org/10.1016/j.scitotenv.2023.164373

Pebesma, E., & Bivand, R. (2025). Spatial data science. https://r-spatial.org/book/

R Core Team. (2024). R: A language and environment for statistical computing. Vienna, Austria: R Foundation for Statistical Computing. https://www.R-project.org/

Raymond, P. A., & Cole, J. J. (2001). Gas exchange in rivers and estuaries: Choosing a gas transfer velocity. *Estuaries*, *24*(2), 312–317. https://doi.org/10.2307/1352954

Raymond, P. A., Hartmann, J., Lauerwald, R., Sobek, S., McDonald, C., Hoover, M., et al. (2013a). Global carbon dioxide emissions from inland waters. *Nature*, *503*(7476), 355–359. Article 7476. https://doi.org/10.1038/nature12760

Raymond, P. A., Hartmann, J., Lauerwald, R., Sobek, S., McDonald, C., Hoover, M., et al. (2013b). Global carbon dioxide emissions from inland waters. *Nature*, *503*(7476), 355–359. Article 7476. https://doi.org/10.1038/nature12760

Raymond, P. A., Zappa, C. J., Butman, D., Bott, T. L., Potter, J., Mulholland, P., et al. (2012). Scaling the gas transfer velocity and hydraulic geometry in streams and small rivers. *Limnology and Oceanography: Fluids and Environments*, *2*(1), 41–53. https://doi.org/10.1215/21573689-1597669

Regnier, P., Resplandy, L., Najjar, R. G., & Ciais, P. (2022). The land-to-ocean loops of the global carbon cycle. *Nature*, *603*(7901), 401–410. https://doi.org/10.1038/s41586-021-04339-9

Riveros-Iregui, D. A., Covino, T. P., & González-Pinzón, R. (2018). The importance of and need for rapid hydrologic assessments in Latin America. *Hydrological Processes*, *32*(15), 2441–2451. https://doi.org/10.1002/hyp.13163

Rocher-Ros, G., Sponseller, R. A., Lidberg, W., Mörth, C.-M., & Giesler, R. (2019). Landscape process domains drive patterns of CO2 evasion from river networks. *Limnology and Oceanography Letters*, *4*(4), 87–95. https://doi.org/10.1002/lol2.10108

Saccardi, B., & Winnick, M. (2021). Improving predictions of stream CO2 concentrations and fluxes using a stream network model: A case study in the east river watershed, CO, USA. *Global Biogeochemical Cycles*, *35*(12), e2021GB006972. https://doi.org/10.1029/2021GB006972

Sander, R. (2023). Compilation of Henry's law constants (version 5.0.0) for water as solvent. *Atmospheric Chemistry and Physics*, *23*(19), 10901–12440. https://doi.org/10.5194/acp-23-10901-2023

Sawakuchi, H. O., Neu, V., Ward, N. D., Barros, M. d. L. C., Valerio, A. M., Gagne-Maynard, W., et al. (2017). Carbon dioxide emissions along the lower Amazon river. *Frontiers in Marine Science*, *4*. https://doi.org/10.3389/fmars.2017.00076

Schelker, J., Singer, G. A., Ulseth, A. J., Hengsberger, S., & Battin, T. J. (2016). CO2 evasion from a steep, high gradient stream network: Importance of seasonal and diurnal variation in aquatic pCO2 and gas transfer. *Limnology & Oceanography*, *61*(5), 1826–1838. https://doi.org/10.1002/lno.10339

Schneider, C. L., Herrera, M., Raisle, M. L., Murray, A. R., Whitmore, K. M., Encalada, A. C., et al. (2020). Carbon Dioxide (CO2) fluxes from terrestrial and aquatic environments in a high-altitude tropical catchment. *Journal of Geophysical Research: Biogeosciences*, *125*(8), e2020JG005844. https://doi.org/10.1029/2020JG005844

Taillardat, P., Bodmer, P., Deblois, C. P., Ponçot, A., Prijac, A., Riahi, K., et al. (2022). Carbon dioxide and methane dynamics in a peatland headwater stream: Origins, processes and implications. *Journal of Geophysical Research: Biogeosciences*, *127*(7), e2022JG006855. https://doi.org/10.1029/2022JG006855

Teodoru, C. R., del Giorgio, P. A., Prairie, Y. T., & Camire, M. (2009). Patterns in pCO2 in boreal streams and rivers of northern Quebec, Canada. *Global Biogeochemical Cycles*, *23*(2). https://doi.org/10.1029/2008GB003404

Ulseth, A. J., Hall, R. O., Boix Canadell, M., Madinger, H. L., Niayifar, A., & Battin, T. J. (2019). Distinct air–water gas exchange regimes in low- and high-energy streams. *Nature Geoscience*, *12*(4), 259–263. Article 4. https://doi.org/10.1038/s41561-019-0324-8

Wallin, M., Buffam, I., Öquist, M., Laudon, H., & Bishop, K. (2010). Temporal and spatial variability of dissolved inorganic carbon in a boreal stream network: Concentrations and downstream fluxes. *Journal of Geophysical Research*, *115*(G2). https://doi.org/10.1029/2009JG001100

Wallin, M. B., Campeau, A., Audet, J., Bastviken, D., Bishop, K., Kokic, J., et al. (2018). Carbon dioxide and methane emissions of Swedish low-order streams—A national estimate and lessons learnt from more than a decade of observations. *Limnology and Oceanography Letters*, *3*(3), 156–167. https://doi.org/10.1002/lol2.10061

Wallin, M. B., Öquist, M. G., Buffam, I., Billett, M. F., Nisell, J., & Bishop, K. H. (2011). Spatiotemporal variability of the gas transfer coefficient (KCO2) in boreal streams: Implications for large scale estimates of CO2 evasion. *Global Biogeochemical Cycles*, *25*(3). https://doi.org/10.1029/2010GB003975

Wanninkhof, R. (2014). Relationship between wind speed and gas exchange over the ocean revisited. *Limnology and Oceanography: Methods*, *12*(6), 351–362. https://doi.org/10.4319/lom.2014.12.351

Whitmore, K., Riveros-Iregui, D., Farquhar, E., DelVecchia, A. G., Rocher-Ros, G., & Suárez, E. (2024). Carbon evasion dynamics in a tropical, high-elevation, peatland ecosystem are mediated by watershed morphology [Dataset]. *HydroShare*. https://doi.org/10.4211/hs.5b7f7c870eed4f8591bc8be01b34ee54

Whitmore, K. M., Stewart, N., Encalada, A. C., Suárez, E., & Riveros-Iregui, D. A. (2021). Spatiotemporal variability of gas transfer velocity in a tropical high-elevation stream using two independent methods. *Ecosphere*, *12*(7), e03647. https://doi.org/10.1002/ecs2.3647

Wickham, H. (2009). Introduction. In H. Wickham (Ed.), *Ggplot2: Elegant graphics for data analysis* (pp. 1–7). Springer. https://doi.org/10.1007/978-0-387-98141-3_1

Woodrow, R. L., White, S. A., Conrad, S. R., Wadnerkar, P. D., Rocher-Ros, G., Sanders, C. J., et al. (2024). Enhanced stream greenhouse gas emissions at night and during flood events. *Limnology and Oceanography Letters*, *9*(3), 276–285. https://doi.org/10.1002/lol2.10374

Zappa, C. J., McGillis, W. R., Raymond, P. A., Edson, J. B., Hintsa, E. J., Zemmelink, H. J., et al. (2007). Environmental turbulent mixing controls on air-water gas exchange in marine and aquatic systems. *Geophysical Research Letters*, *34*(10). https://doi.org/10.1029/2006GL028790